04,07

Medium-density amorphous ice obtained by decay of water-helium gel

© V.V. Sinitsyn[1,2], O.G. Rybchenko[1,2], V.B. Efimov[1], A.A. Viryus[3]

[1] Institute of Solid State Physics, Russian Academy of Sciences, Chernogolovka, Moscow distr., Russia
[2] National Research University Higher School of Economics, Moscow, Russia
[3] Institute of Experimental Mineralogy, Russian Academy of Sciences, Chernogolovka, Moscow distr., Russia

E-mail: sinitsyn@issp.ac.ru

Received June 8, 2023
Revised June 26, 2023
Accepted June 28, 2023

The article presents experimental studies of structural changes that occur during heating of nanosized powders of amorphous ice obtained by decay of a water-helium gel. Thermal annealing of the obtained samples was carried out by short exposures (about 15 minutes) at different temperatures in the range of 110−230 K. The behavior of the amorphous phase during annealing was analyzed within the framework of its description by a mixture of amorphous ices of low and medium density (*LDA* and *MDA*, respectively). It was found that at the such description, the virgin sample was predominantly in the *MDA* state, while the proportion of the *LDA* phase was about 7 times less ($MDA/LDA \approx 7:1$). It has been established that during annealing, a multistage process of structural transformations of the initial $LDA + MDA$ sample takes place: from initial changes in the amorphous state at 110 K through crystallization of the cubic ice phase I_c with its intensive growth at a temperature of 130 K to the transformation of cubic ice into the hexagonal phase I_h in the temperature range $T = 135-230$ K.

Keywords: ice, amorphous state, crystallization, medium density amorphous ice, impurity-helium gels, X-ray diffraction analysis.

DOI: 10.61011/PSS.2023.08.56569.103

1. Introduction

Currently, several methods have been developed to obtain amorphous ice from all three aggregate states of H_2O: gaseous (steam) [1], liquid (water) [2–8] and crystalline (hexagonal ice I_h and high pressure ice VIII) [9–16]. The existence of amorphous ice was first discovered in 1935, when Barton and W.F.Oliver conducted studies of samples obtained by spraying water vapor onto a substrate cooled to boiling points of liquid nitrogen [1]. This ice has the abbreviation *ASW* (*amorphous solid water*) in literature. On the other hand, it is well known that many liquids, when cooled at speeds above a certain critical, turn into glass (an amorphous state obtained by quenching the corresponding liquid). However, it was not possible to vitrify the water for a long time, despite that it can be relatively easily supercooled at $\sim 15-20$ degrees below the melting point. It turned out that it is necessary to cool down water at extremely high speeds $> 10^5$ K/s for its vitrification [3,4]. This cooling process is called „hyperquenching“ in the literature, and the resulting amorphous ice — *hyperquenching glassy water* (*HGW*) [3–8]. Many physical properties of states *ASW* and *HGW* like density, thermal stability region, structural factors of X-ray and neutron scattering are close, their density is 0.94 g/cm^3 and these ices are classified as amorphous low density ice (*LDA*) [7,17–20].

The possibility of obtaining amorphous ice from the crystalline phase was first demonstrated in [9]. The authors of [9] experimentally showed that when crystal ice I_h is compressed at temperatures ~ 77 K and pressure $\sim 1.1-1.2$ GPa, it leaded to amorphization of a sample with a density of 1.15−1.17 g/cm^3 [10,21,22]. The amorphous ice formed as a result of this „cold melting“ turned out to be almost 20% denser than the *LDA* modification and was called „amorphous ice of high density“ (*HDA*) [9–11]. When this amorphous ice was heated above $T \sim 117$ K at 1 atm, a transition to a less dense modification was observed, which corresponds to the *LDA* phase [9,10,11,19]. Moreover, if this phase *LDA* was then compressed with a pressure $P \sim 0.3$ GPa at $T \sim 130$ K, there was a first order phase transition to the state *HDA*, which reversibly returned to *LDA* when the pressure was isothermally released below ~ 0.05 GPa [20]. It was possible to obtain even denser amorphous phases by various heat treatments of the *HDA* state [23,24].

Recently, another form of amorphous ice was discovered, which was obtained by prolonged (more than 40 h) grinding of crystalline ice I_h at the boiling point of liquid nitrogen (~ 77 K) and was called „amorphous ice of medium density“ (*MDA*) [25]. The obtained samples, along with the amorphous phase *MDA*, contained a large amount of residual hexagonal ice. Studies have shown that the

density of *MDA* ice is $\sim 1\,g/cm^3$ and when it is heated, a phase transition occurs into I_h crystalline phase ($T \sim 150\,K$, 1 atm) with thermal effect $\sim 1.21\,kJ/mol$. Ice *MDA* ($T \sim 77\,K$) transfers to the *HDA* phase at approximately the same pressures as ice I_h during its compression but with a slightly smaller volume surge. Structural studies show that the position of the first halo of *MDA* of ice on at X-ray CuK_α is approximately at $2\Theta \approx 27\,grad$, which is closer to the position of the first halo for *HDA* phase ($2\Theta \geq 28\,grad$) [8,9,18,25] than to *LDA* ($2\Theta \approx 24\,grad$) [7–9,18,26,27]. However, in the spectra of inelastic light scattering (Raman spectroscopy), the position of the frequencies of the O-H longitudinal mode for *MDA* ice turns out to be closer to the spectrum of *LDA*, and not *HDA* ice [25]. The authors assumed that the *MDA* state corresponds to the structure of water under normal conditions.

The structural features of water can be studied *in situ* in its equilibrium state [28,29], or it possible to try to freeze the structure of the equilibrium state by performing ultrafast quenching and study it on the resulting amorphous ice. One of the ways to obtain ice samples in an amorphous state is the technique of formation nanoscale samples with the decay of impurity-helium gels [30]. The process essentially comprises a rapid quenching of a mixture of a small amount of water vapor (as an impurity) with a large amount of gaseous helium, as a medium, to a temperature of 1.6 K. In this case, clusters of water molecules are formed, surrounded by a large number of helium atoms. The presence of a helium environment around polar molecules H_2O prevents the crystallization of water and leads to the formation of a water-helium gel consisting of particles with a size of 30–60 nm, which, after warming to nitrogen temperatures and sublimation of helium atoms, turns into amorphous ice [31]. Thus, the samples of amorphous ice obtained by the described method (hereinafter referred to as *NPA — nano particle amorphous* ice) are a powder of nanoscale particles with a developed free surface. The formation of amorphous ice nanoparticles through impurity-helium gel can be considered as a simulation of amorphization processes occurring with free water clusters in the upper layers of atmosphere, or, given the temperature of the cosmic microwave background and the dominant number of light atoms in interstellar space, as a simulation of the formation of ice clusters in outer space.

In this regard, a detailed structural analysis of amorphous samples obtained during the decay of a helium gel and the study of phase transformations occurring in them during heating were of interest. Such studies were completed in this work and it was shown that the nanoscale amorphous ice obtained in this way corresponds to a greater extent to the *MDA* state.

2. Experimental methods and samples

The original samples of amorphous ice *NPA* were obtained using the impurity-helium gel decay method described above. This method was also used in the works [30–36]. The technology of ice sample synthesis *NPA* is described in more detail in [30–32]. The proportion of water vapor in the water-helium mixture cooled to the temperature of superfluid helium was ~ 2–3%. The indicated concentration of water vapor in the flow of gaseous helium was obtained by bubbling helium through distilled water, and the vapor pressure of the gas mixture at room temperature was 18–22 Torr. Then the water-helium mixture was introduced through a special glass filling tube ($D = 1.5\,cm$), the end of which was in the superfluid helium at a depth of $\sim 1\,cm$ (the temperature of the superfluid helium is 1.6 K). The mixture cooled in this way condensed into a gel and settled at the bottom of the quartz ampoule. The preparing gel consists of conglomerates of polar water molecules surrounded by localized helium atoms. The rate of condensation of particles of a mixture of water and helium into the gel was of the order of 10^{20} atoms (molecules)/s, the concentration of water molecules in the gel reached a value of several percent. The cooling rate of the water-helium mixture, estimated by the time of passing of the mixture along the filling tube with a temperature gradient from 300 K to ≈ 1 K, was of the order of 1000 K/s. Amorphous ice powder after helium sublimation from the sample was moved from the helium dewar for a time of 3–5 seconds to liquid nitrogen, where the sample was stored until X-ray measurements.

Low-temperature diffraction measurements were carried out on a Siemens D500 X-ray diffractometer using CuK_α-radiation in a CRYO205S nitrogen X-ray cryostat. The combined system for adjusting the flow of nitrogen gas and heating the sample holder provided high accuracy of temperature control and stabilization. The sample was loaded through the side flange of the diffraction chamber. This scheme allows to quickly, in less than ten seconds, perform cold loading of a sample on a silicon substrate from a bath with liquid nitrogen into the working chamber of the cryostat. The temperature of the sample holder did not rise above 85 K. The depth of the recess with a diameter of 10 mm in the silicon substrate where the powdered sample was placed was 0.3 mm.

The impact of annealing modes on structural changes was studied by sequentially increasing the sample temperature to the annealing temperature and holding the sample under these conditions for a controlled time (usually 15 min), followed by cooling to the measurement temperature. The annealing temperature was maintained with an accuracy of ± 1 K. The duration of X-ray scanning was in the order of several hours, X-ray examinations were carried out at a temperature close to nitrogen ($T_{X\text{-}Ray} \approx 85\,K$). This temperature was chosen to avoid possible structural changes during X-ray studies, since our previous data [33,34] showed high structural stability of samples of nanocluster amorphous ice at liquid nitrogen temperature. The annealing procedure was repeated at a higher temperature after the X-ray measurement. X-ray spectra were processed by using the TOPAS program.

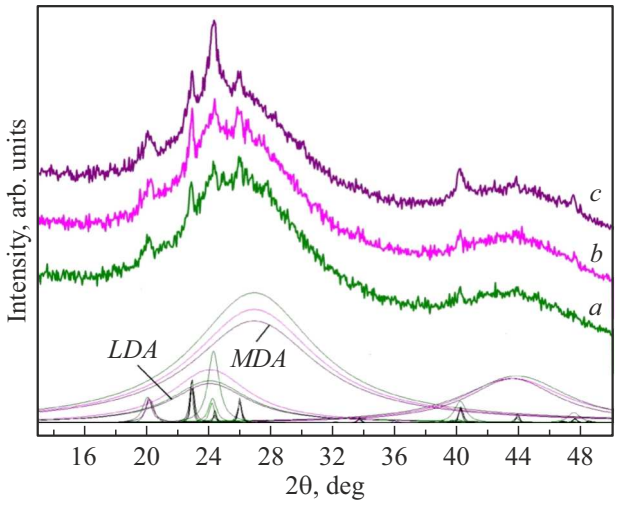

Figure 1. X-ray scattering spectra *NPA* of ice: initial (a), after annealing at 110 K (b) and 120 K (c); thin lines of the same colors show the decomposition of experimental halos into components *LDA* and *MDA*; the background curve is not shown so as not to clutter the drawing, the crystal lines correspond to I_h and I_c ice.

3. Experimental results

The X-ray scattering spectra of the initial sample at a temperature of 85 K, as well as when it is successively heated to temperatures of 110 and 120 K are shown in Fig. 1. It can be seen that all the studied spectra contain weak crystal reflexes except for two amorphous halos. The analysis shows that these reflections belong to the crystalline phases — hexagonal I_h and cubic I_c ice, which apparently formed from water vapor in the laboratory air during the transfer of the sample to the cryostat working chamber. The total fraction of crystalline phases in the initial sample does not exceed 5%. The intensity of crystal reflexes when the sample is heated to 110 K practically does not change (Fig. 1, *a, b*). In addition, the X-ray images of all samples contain one or two weak peaks in the area of diffraction angles 19−20°, which cannot be identified either as known crystalline phases of ice or as known crystalline clathrates of helium and nitrogen. These lines disappear after annealing the sample at 230 K. The nature of these lines requires additional research.

The positions of the amorphous halos on the spectrum of the initial sample are $2\theta \approx 26°$ and 43.5° for the 1st and 2nd halos, respectively. According to numerous studies, the position of the first halo for *LDA* ice in X-ray CuK_α-radiation is $2\theta \approx 24°$ [7,8,9,18,24,26] for *HDA* ice $2\theta \geq 28°$ [8,9,18,25,27], and for the recently opened *MDA* ice $2\theta \approx 27.2°$ [25].

Given the method of obtaining samples of *NPA* ice, it is natural to expect that its structure is close to *LDA*. However, the position of the halo in our case differs significantly from the value known from the literature for *LDA* ice in the direction of large scattering angles. This can be explained based on the assumption that the resulting amorphous state is a mixture of two amorphous modifications, one of which is low-density ice *LDA*, and the second modification has a higher density. We believe that such a situation may occur, since the fundamental possibility of simultaneous coexistence of two amorphous phases in the sample, as well as the transformation of one of these forms into another, has been repeatedly shown by the example of ice of different densities in works devoted to the study of ice polyamorphism at high pressures [37,38].

Figure 1 shows a method for describing the X-ray spectra of the sample *NPA* under the assumption of a two-amorphous state with a small fraction of crystalline $(I_h + I_c)$ inclusions for the initial sample, as well as for samples after exposure at 110 and 120 K; thin lines show the decomposition of the first an amorphous halo into two fractions. During decomposition, the position of the halo for the *LDA* modification was fixed at the value of $2\theta = 24°$, which corresponds to the literature data. The position of the halo for the second amorphous phase was determined by decomposing the spectrum of the initial sample from the condition of minimizing the deviation between the calculated and experimental curves. As a result of this decomposition, it turned out that the ratio of the fractions of amorphous phases in the initial sample is approximately $MDA/LDA \approx 7:1$ (with the proportion of crystalline inclusions $\sim 5\%$).

The halo position determined in this way for the second amorphous phase ($2\theta \approx 26.8°$) turned out to be very close to the value for *MDA* ice according to [25] ($2\theta \approx 27.2°$). A slight difference in these values, indicating a lower density of the amorphous ice obtained by us compared to *MDA* ice, may be due to the nanoscale nature of the powder *NPA* (30−60 nm). Such a significant decrease in particle size can lead to a change in intermolecular distances in *NPA* samples with a large proportion of near-surface molecules, that is, to a decrease in density.

Thus, the analysis of experimental data suggests that the sample synthesized during the decay of a water-helium gel consists of two phases of amorphous ice, while the majority ($\sim 83\%$) is ice of medium density *MDA*. At the same time, the ratio of the fractions of amorphous phases for the initial sample is approximately $MDA/LDA \approx 7:1$ (with the proportion of crystalline inclusions $\sim 5\%$).

After annealing of the initial sample at a temperature of $T = 110$ K, the position of the 1st amorphous halo shifts to the region of small angles by about 0.3° with a very slight decrease in its half-width. This can be explained by a partial transformation of $MDA \rightarrow LDA$. A similar transformation of one amorphous modification into another one is observed when heating high-density ice (*HDA*) and its transition to *LDA*. Indeed, at fixed positions of the halo maxima for two amorphous phases at $2\theta = 24°$ (*LDA*) and $2\theta = 26.8°$ (*MDA*), the displacement of the total halo towards small scattering angles means a change in the ratio of the fractions of its two components: the amount of amorphous ice of medium density *MDA* decreases, and the amount of *LDA*

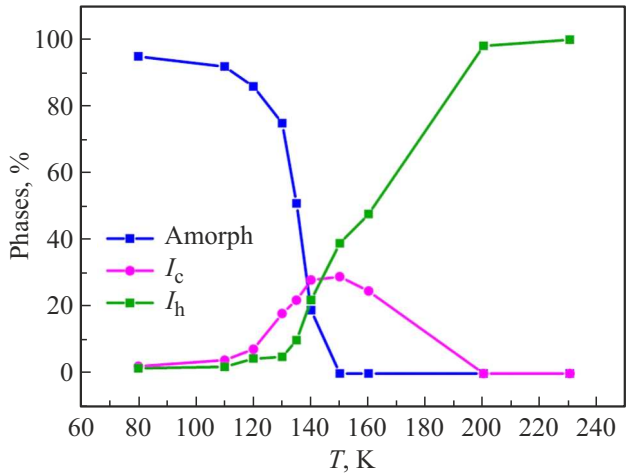

Figure 2. Dependences of the total fraction of amorphous ($LDA + MDA$) and fractions of crystalline phases (I_h and I_c) on the annealing temperature.

increases slightly (Fig. 1, *a, b*). The relaxation process may be another explanation for this behavior of the amorphous component of the sample. A slight shift of the amorphous halo *MDA* of ice towards smaller scattering angles was also observed at the initial stages of heating in the work [25]. Note that at this stage of annealing of the amorphous phase, other processes may occur that lead to the displacement of the total amorphous halo, for example, relaxation of the amorphous state or the final removal of residual helium from the *NPA* sample, which may also slightly change its density. Therefore, additional more detailed studies of the kinetics of transformation are required to make any final conclusions about the nature of the observed weak changes in the content of the amorphous fraction in the *NPA* sample at 110 K.

The total content of amorphous phases decreases somewhat (Fig. 1, *c*) at an annealing temperature of 120 K and cubic ice I_c begins to form, but its fraction, and hence the crystallization rate is still small. At the same time, the shape and position of the total amorphous halo continue to change: with a slight decrease in the amount of amorphous phase in the sample (after annealing at 120 K by about 7%), the maximum of the halo noticeably shifts towards small scattering angles (Fig. 1, *a*).

It should be noted that it is necessary to know the exact parameters of their halos obtained experimentally for each modification separately to conduct a quantitative analysis of the ratio of two amorphous phases, which is not possible to do in our case. In addition, the formation of very small crystallites at the initial stage of crystallization of cubic ice I_c can make some contribution to the displacement of the total amorphous halo towards smaller angles, since its line (111) at the position $2\theta \sim 24.25^\circ$ coincides with the small-angle part of the halo. Thus, this transformation also introduces an error in estimating the amount of *LDA* phase in the presence of a crystallization process in the sample. Given these circumstances, the proportions of amorphous phases and their change with temperature can only be assessed qualitatively. In this regard, Figure 2 shows the dependence on the annealing temperature of only the total amount of amorphous fraction ($LDA + MDA$), and also shows the change in the fractions of crystalline phases.

The X-ray scattering spectrum of the studied sample annealed at temperatures of 130, 135 and 140 K is shown in Fig. 3. At a temperature of 130 K, the crystallization process of the sample accelerates with the formation of cubic ice I_c (its fraction reaches $\sim 18\%$ of the entire sample, Fig. 2) and a decrease in the proportion of the amorphous component. During the exposure of the samples at $T = 135$ and 140 K (Fig. 3, green and blue curves, respectively), two parallel processes occur in the crystalline phases: the formation of I_c (new small crystallites appear from the amorphous phase and previously formed ones grow) and the transformation of cubic ice into hexagonal $I_c \rightarrow I_h$ begins.

After annealing at 140 K, the content of the phase I_h is already $\sim 22\%$, and of cubic ice $I_c \sim 28\%$ (Fig. 2). The amount of amorphous fraction decreases significantly, although it does not disappear completely. At the same time, during exposure at $T = 135$ K, more complex processes occur in it: the amount of phase *MDA* decreases, and instead of the halo *LDA*, some substrate appears („pedestal“) under the peaks of crystalline phases. This feature of changing the diffraction pattern during the crystallization of amorphous ice was also considered in [13,37]. The mechanism of the initial stages of crystallization at this temperature can be explained as follows. It is known that at the glass transition temperature $T_g = 136$ K, an endothermic transition occurs from „frozen“ amorphous to an ultra-viscous liquid state [7,8,18]. Therefore, it can be assumed that the observed amorphous „pedestal“ in the X-ray scattering spectrum at a temperature of 135 K is associated with this transition. Then, very small (< 5 nm) crystallites with a small amount of amorphous matrix between them are formed after cooling the ultra-viscous liquid from the annealing temperature (~ 135 K) to the X-ray measurement temperature (85 K). The existence of such a „intermediate“ phase was proposed in [37], where this state was designated as „restrained“ amorphous phase (I_{ar}). In this case, the nanocrystalline fraction can be nanocrystals I_c containing crystallographic defects in the form of hexagonal interlayers or a mixture of nanoscale nuclei of two crystalline phases I_c and I_h simultaneously. In our case, a significant part of the resulting nanocrystals should have a structure close to hexagonal ice, as evidenced by the subsequent intensive growth of the lines I_h at 140 K (Fig. 3, blue curve).

A further increase in temperature continues the crystallization process (Fig. 4). On the spectra of the studied samples after annealing at 150 and 160 K, the lines of crystalline phases are located on a still noticeable „pedestal“ corresponding to „restrained“ amorphous phase I_{ar}. Finally, cubic ice turns into hexagonal ice only at temperatures

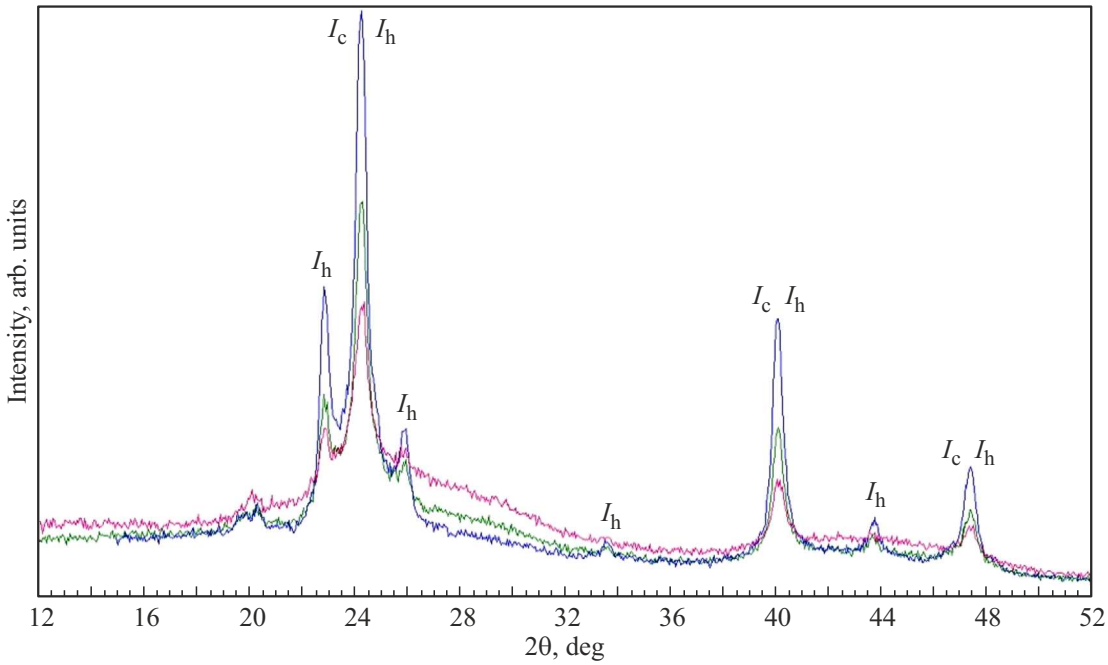

Figure 3. The X-ray scattering spectrum of ice during annealing at: 130 K — red curve; 135 K — green curve; 140 K — blue curve.

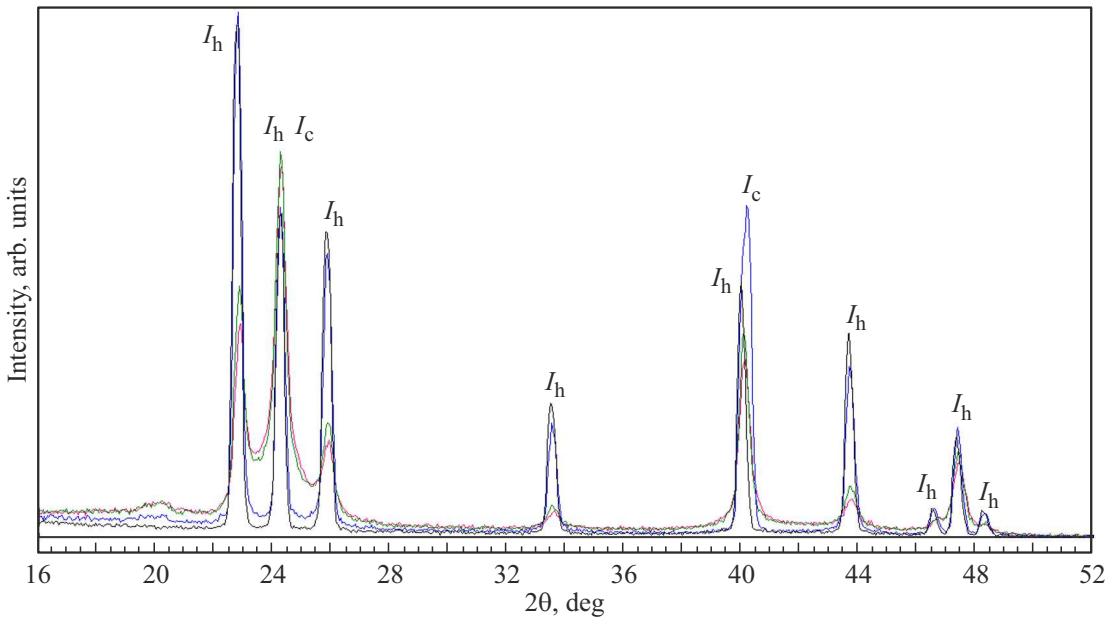

Figure 4. Diffractogram of the sample after annealing at temperatures: red — 150 K, green — 160 K, blue — 200 K, black — 230 K.

above 200 K. Annealing at 230 K completes the transformation of $I_c \rightarrow I_h$ and leads to the disappearance (within experimental error limits) of the disordered component. The sizes of the forming crystallites I_h of ice ($\sim 30-40$ nm) correspond to the sizes of nanoparticles *NPA* derived from experiments on small-angle neutron scattering [31]. The observed structural behavior of the sample under study corresponds well to the calorimetry data of *MDA* and *LDA* phases [18,25].

4. Discussion

Annealing of the initial sample carried out at a temperature of 110 K leads, at first glance, to a slight change in the ratio of *MDA* and *LDA* modifications, i. e. the transformation of *MDA* ice into *LDA*. However, as mentioned above, it is impossible to obtain an exact quantitative ratio of two amorphous fractions, due to the large error in their determination. In addition, other processes may take

place at the initial stages of annealing of the amorphous phase that lead to a displacement of the total amorphous halo, for example, relaxation of the amorphous state or the final removal of residual helium from the *NPA* sample, which may also slightly change its density. Thus, additional more detailed studies are required to clarify the nature of the observed weak changes in the amorphous fraction of samples *NPA* at the initial stage of annealing.

The results of our X-ray studies can be interpreted within the framework of the structure proposed by the authors [25] *MDA* of a state close to the structure of water under normal conditions, given that the main amorphous halo in our studies ($2\theta \approx 26.8^\circ$) and in the work [25] ($2\theta \approx 27.2^\circ$) are close. Within the framework of this interpretation, the amorphous component of the sample consists of two amorphous phases — *LDA* and *MDA*, and the proportion of the last one is at least 83%. X-ray studies performed during annealing of the obtained sample allowed establishing that the *MDA* phase in our experiments persists at 120, 130, 135 and 140 K (Figs. 1 and 3) and finally disappears only after annealing of the sample at 150 K (Fig. 4, *a*). These results are in good agreement with the calorimetric data of [25]. Moreover, a decrease in the amount of *MDA* phase correlates well with an increase in the proportion of cubic ice I_c, while the amount of *LDA* remains almost unchanged (within error limits) during annealing of the sample to a temperature up to 135 K. This suggests that two parallel processes occur in the *NPA* sample: crystallization of *MDA* ice through the formation of a cubic phase into a hexagonal one and the transformation of *LDA* when the temperature $T = 135$ K into a „restrained" I_{ar} phase with subsequent crystallization.

It should be noted here that some change in the short-range order of the H_2O molecules located near the boundary of the powders may take place due to the nanoscale state of the powder in the obtained *NPA* sample, compared with the volume. At the same time, the resulting modification of *NPA* amorphous ice in the structure of an amorphous grid may be a kind of intermediate state between the grids of *LDA* and *MDA* phases with a near-order varying in particle depth, and not a mixture of two separate phases. However, it is important to emphasize that even in this case, most of the amorphous structure of the *NPA* sample is close to amorphous ice of medium density.

Heating of the resulting amorphous sample above 140 K leads to a significant decrease in the proportion of the entire amorphous component in the sample and the growth of crystals at first cubic I_c, then hexagonal I_h phases of ice. Qualitatively, the crystallization process of amorphous samples from water-helium gels turned out to be similar to the phase transformations observed earlier and described in the literature for other amorphous water ice when heated above 135–140 K [8,10,13,16,18,21,24,27,37].

In general, the data obtained data correlate well with the results of [25]. The kinetics of phase transitions for amorphous ice obtained by grinding (strong plastic deformation) and samples obtained from water-helium gel may differ due to the difference in the size of conglomerate particles (tens of microns for grinding and tens of nanometers for the gel decay method) and the presence of a large amount of residual hexagonal ice (tens of percent) in the method grinding.

5. Conclusion

Structural transformations at the process of annealing of a nanoscale ($\sim 30-60$ nm) amorphous ice powder obtained as a result of the decay of a water-helium gel (*NPA*) have been studied. A feature of this method is the quenching of a mixture of water vapor in a large amount of gaseous helium on the surface of superfluid helium. The results of the X-ray studies were interpreted on the basis of a new phase of medium-density amorphous ice (*MDA*) proposed by the authors [25], close to the structure of water under normal conditions. It was found that within the framework of such an approach, the proportion of the *MDA* phase in the obtained sample is more than 80%, the rest of the sample is *LDA* ice, as well as traces of cubic and hexagonal crystalline ice, with a total amount of about 5%, which is significantly lower fractions of crystalline ice obtained by grinding [25].

Heating of the resulting amorphous (*NPA*) sample leads to a decrease in the proportion of the amorphous component and the formation at first of cubic I_c, then hexagonal I_h phases of ice. Crystallization occurs through the formation of an intermediate amorphous-nanocrystalline state, called in the literature „restrained" phase (I_{ar}).

It was found that the crystallization process of amorphous samples obtained from water-helium gels turned out to be similar to the phase transformations observed earlier and described in the literature in amorphous ices obtained by other methods.

Funding

The study was carried out according to the state assignment of the ISSP RAS. V.V. Sinitsyn thanks the scientific and educational project of the Higher School of Economics (No. 23-00-001) for financial support.

Conflict of interest

The authors declare that they have no conflict of interest.

References

[1] E.F. Burton, W.F. Oliver. Proc. R. Soc. Lond. A **153**, 166 (1935).
[2] P. Brüggeller, E. Mayer. Nature **288**, 569 (1980).
[3] G.P. Johari, A. Hallbrucker, E. Mayer. Nature **330**, 552 (1987).
[4] G.P. Johari, A. Hallbrucker, E. Mayer. Science **273**, 90 (1996).
[5] A. Hallbrucker, E. Mayer, G.P. Johari. Phil. Mag. B **60**, 179 (1989).

[6] J.P. Johari, A. Hallbrucker, E. Mayer. J. Chem. Phys. **92**, 6742 (1990).
[7] A. Hallbrucker, E. Mayer, G.P. Johari. J. Chem. Phys. **93**, 4986 (1989).
[8] I. Kohl, L. Bachmann, A. Hallbrucker, E. Mayera, T. Loerting. Phys. Chem. Chem. Phys. **7**, 3210 (2005).
[9] O. Mishima, L.D. Calvert, E. Whalley. Nature **310**, 393 (1984).
[10] E. Whalley. J. Less-Common Met. **140**, 361 (1988).
[11] O. Mishima, L.D. Calvert, E. Whalley. Nature **314**, 76 (1985).
[12] D.D. Klug, Y.P. Handa, J.S. Tse, E. Whalley. J. Chem. Phys. **90**, 2390 (1989).
[13] A.M. Balagurov, O.I. Barkalov, A.I. Kolesnikov, G.M. Mironova, E.G. Ponyatovskii, V.V. Sinitsyn, V.K. Fedotov. JETP Lett. **53**, 30 (1991).
[14] V.V. Sinitsyn, A.I. Kolesnikov. High Press. Res. **9**, 225 (1991).
[15] Koichiro Umemoto, Renata M. Wentzcovitch. Phys. Rev. B **69**, 180103 (2004).
[16] O. Mishima. Proc. Jpn. Acad. B **86**, 165 (2010).
[17] M.C. Bellissent-Funel, L. Bosio, A. Hallbrucker, E. Mayer, R. Sridi-Dorbez. J. Chem. Phys. **97**, 1282 (1992).
[18] T. Loerting, N. Giovambattista. J. Phys.: Condens. Matter. **18**, R919 (2006).
[19] T. Loerting, K. Winkel, M. Seidl, M. Bauer, Ch. Mitterdorfer, Ph.H. Handle, Ch.G. Salzmann, E. Mayer, J.L. Finney, D.T. Bowron. Phys. Chem. Chem. Phys. **13**, 8783 (2011).
[20] O. Mishima. J. Chem. Phys. **100**, 5910 (1994).
[21] O.V. Stalgorova, E.L. Gromnitskaya, V.V. Brazhkin, A.G. Dyapin. Pis'ma v ZhETF **69**, *9*, 653 (1999). (in Russian).
[22] E.L. Gromnitskaya, A.G. Dyapin, O.V. Stalgorova, I.V. Danilov, V.V. Brazhkin. Pis'ma v ZhETF **96**, *12*, 879 (2012). (in Russian).
[23] R.J. Nelmes, John S. Loveday, Thierry Strässle, Craig L. Bull, Malcolm Guthrie, Gérard Hamel, Stefan Klotz. Nature Phys. **2**, 414 (2006).
[24] T. Loerting, C. Salzmann, I. Kohl, E. Mayer, A. Hallbrucker. Phys. Chem. Chem. Phys. **3**, 5355 (2001).
[25] Alexander Rosu-Finsen, Michael B. Davies, Alfred Amon, Han Wu, Andrea Sella, Angelos Michaelides, Christoph G. Salzmann. Science **379**, 474 (2023).
[26] M.S. Elsaesser, K. Winkel, E. Mayer, T. Loerting. Phys. Chem. Chem. Phys. **12**, 708 (2010).
[27] T. Loerting, C. Salzmann, I. Kohl, E. Mayer, A. Hallbrucker. Phys. Chem. Chem. Phys. **3**, 5355 (2001).
[28] Ph. Wernet, D. Nordlund, U. Bergmann, M. Cavalleri, M. Odelius, H. Ogasawara, L.Å. Näslund, T.K. Hirsch, L. Ojamäe, P. Glatzel, L.G.M. Pettersson, A. Nilsson. Science **304**, 995 (2004).
[29] C. Huang, K.T. Wikfeldt, T. Tokushima, D. Nordlund, Y. Harada, U. Bergmann, M. Niebuhr, T.M. Weiss, Y. Horikawa, M. Leetmaa, M.P. Ljungberg, O. Takahashi, A. Lenz, L. Ojamäe, A.P. Lyubartsev, S. Shin, L.G.M. Pettersson, A. Nilsson. PNAS **106**, 15214 (2009).
[30] V. Efimov, L. Mezhov-Deglin. Patent N 2399581 (2010).
[31] V.B. Efimov, L.P. Mezhov-Deglin, C.D. Dewhurst, A.V. Lokhov, V.V. Nesvizhevsky. Physics ID 808212 (2015). (http://dx.doi.org/10.1155/2015/808212)
[32] L.P. Mezhov-Deglin. Phys.-Usp. **48**, 1061 (2005).
[33] V. Efimov, A. Izotov, L. Mezhov-Deglin, V. Nesvizhevskii, O. Rybchenko, A. Zimin. Low Temper. Phys. **41**, 603 (2015).
[34] V.B. Efimov, A.N. Izotov, A.A. Levchenko, L.P. Mezhov-Deglin, S.S. Khasanov. JETP Lett. **94**, 621 (2011).
[35] V.B. Efimov, L.P. Mezhov-Deglin, O.G. Rybchenko. Low Temper. Phys. **46**, 155 (2020).
[36] L.P. Mezhov-Deglin, A.M. Kokotin. JETP Lett. **70**, 756 (1999).
[37] Peter Jenniskens, David F. Blake. Science **265**, 753 (1994).
[38] Philip H. Handle, Thomas Loerting. J. Chem. Phys. **148**, 124508 (2018).

Translated by A.Akhtyamov